A Study on the Selective Organometallic Vapor Deposition of Palladium onto Self-assembled Monolayers of 4,4′-Biphenyldithiol, 4-Biphenylthiol, and 11-Mercaptoundecanol on Polycrystalline Silver

Ulrike Weckenmann,[†] Silvia Mittler,[‡] Stephan Krämer,[‡] Anne K. A. Aliganga,[‡] and Roland A. Fischer*[,†]

Lehrstuhl für Anorganische Chemie II, Ruhr-Universität Bochum, Universitätsstr. 150, 44780 Bochum, Germany, and Max-Planck-Institut für Polymerforschung, Ackermannweg 10, 55128 Mainz, Germany

Received June 12, 2003. Revised Manuscript Received October 30, 2003

The selective organometallic vapor deposition of palladium onto self-assembled monolayers using cyclopentadienyl-allyl-palladium (Cp(allyl)Pd) as the palladium source was investigated by X-ray photoelectron spectroscopy (XPS). It was found that the deposition onto SAMs formed of 4,4′-biphenyldithiol (BDT) on polycrystalline silver substrates proceeds in two successive steps. During the first step, a monolayer of a Pd(II) species is formed selectively on a BDT-SAM whereas no deposition can be observed on a 4-biphenylthiol-SAM (BT). Upon extension of the deposition time, unselective deposition of Pd(0) on the surface of both the Pd(II)-coated BDT-SAM and BT-SAM takes place in a second step. To deposit Pd(0) while maintaining the selectivity of the process, a different approach has been chosen: Trimethylamine alane (TMAA) was deposited selectively on an hydroxy-terminated SAM obtained by self-assembly of 11-mercaptoundecanol on a silver substrate. The resulting surface, which possesses highly reactive Al−H bonds, was exposed to the vapor of Cp(allyl)Pd at room temperature and the deposition of Pd(0) was observed. On a dodecanethiol-SAM, which has been subjected to the same procedure, neither aluminum nor palladium could be detected, proving the selectivity of both the adsorption of TMAA and the deposition of palladium.

Introduction

The growth of thin films and nanostructures of metals and semiconductors plays an important role in many fields of materials science, for example, micro- and optoelectronics, photovoltaics, and hard coatings for wear resistance.[1−4] Over the past 2 decades, chemical vapor deposition (CVD) has attracted increasing interest as an alternative to physical deposition techniques (PVD). The main advantages of CVD over PVD are the conformal coverage, which allows the uniform coating of substrates exhibiting a complex topography, and the possibility of area selective deposition, where nucleation and subsequent growth only occur on so-called growth areas whereas on nongrowth areas nucleation is inhibited and therefore no deposition can be observed.[5,6] The latter aspect is a particularly interesting challenge because it directly addresses the involved precursor chemistry. To achieve the selective deposition of a material, the deposition has to be carried out under kinetically controlled conditions. In classical CVD processes, kinetically stable binary halogenides and hydrides are used (e.g., $TiCl_4$, NH_3, WF_6), which are deposited at high temperatures (>600 °C) near the thermodynamical equilibrium, which limits possible selectivities.[7,8] In contrast, if organometallic precursors are used instead of classical CVD precursors, it is in principle possible to tune the characteristics of the precursor, namely, the volatility, the decomposition temperature, and the reactivity, by variation of the organic ligands surrounding the central metal atom. In addition, it is possible to carry out the deposition at low temperatures in a kinetically controlled regime, which is the essential requirement for the selective deposition of a material.[4,9,10] Furthermore, mild deposition conditions allow the coating of temperature-sensitive substrates (e.g., polymers) and decrease diffusion processes, which makes it possible to generate multilayer structures consisting of distinct ultrathin layers.[2,4]

Following this strategy, we have recently demonstrated the feasibility of selective organometallic CVD

* To whom correspondence should be addressed. E-mail: roland.fischer@ruhr-uni-bochum.de.
† Ruhr-Universität Bochum.
‡ Max-Planck-Institut für Polymerforschung.

(1) *Thin Film Processes II*; Vossen, J. L., Kern, W., Eds.; Academic Press Inc.: New York, 1991.
(2) *Chemical Vapor Deposition, Principles and Applications*; Hitchman, M. L., Jensen, K. F., Eds.; Academic Press: London, 1993.
(3) Pochet, L. F.; Howard, P.; Safaie, S. *Surf. Coat. Technol.* **1997**, *94−95*, 70.
(4) *The Chemistry of Metal CVD*; Kodas, T. T., Hampden-Smith, M. J., Eds.; VCH: Weinheim, 1994.
(5) Gladfelter, W. L. *Chem. Mater.* **1993**, *5*, 1372.
(6) Gates, S. M. *Chem. Rev.* **1996**, *96*, 1519.
(7) McConica, C. M.; Krishnamani, K. *J. Electrochem. Soc.* **1986**, *133*, 2542.
(8) Lifshitz, N.; Williams, D. S.; Capio, C. D.; Brown, J. M. *J. Electrochem. Soc.* **1987**, *134*, 2061.
(9) Jain, A.; Gelatos, A. V.; Kodas, T. T.; Hampden-Smith, M. J.; Marsh, R.; Mogab, C. J. *Thin Solid Films* **1995**, *262*, 52.
(10) Holl, M. M.; Seidler, P. F.; Kowalczyk, S. P.; McFeely, F. R. *Inorg. Chem.* **1994**, *33*, 510.

10.1021/cm031094p CCC: $27.50
Published on Web 01/21/2004

(OMCVD) of ultrathin gold layers onto self-assembled monolayers (SAMs) formed of ω-functionalized aliphatic thiols on gold and silver substrates.[11−13] On the basis of these results, an integrated Mach−Zender interferometer for sensing purposes was developed.[14]

The use of SAMs as substrates for the investigation of the selectivity of an OMCVD process offers several advantages: Their ease of preparation as well as their well-defined structure makes them ideal model substrates.[15,16] Since the chemical and physical properties of a SAM surface mainly depend on the end group of the organic thiol of which the SAM is formed, it is possible to generate a surface with specific properties by modifying the end group of the thiol used for the generation of a SAM.[17] But even apart from the use of SAMs as model substrates, the metallization of SAMs is of great practical interest in the rapidly growing field of nanotechnology.[18−21] The development of active nanodevices, for example, for the construction of molecular computers, essentially relies on the availability of techniques which allow the selective deposition of nanoelectrodes on top of two-dimensionally structured organic layers. OMCVD presents a suitable method for this purpose because it is fully compatible with established manufacturing processes in the microelectronic industry. Our studies have revealed that it is possible to selectively deposit gold via OMCVD onto thiol-terminated SAMs whereas no deposition occurs on hydroxy- and methyl-terminated SAMs. We found that the reaction between the gold precursor (trimethylphosphine)methylgold and the thiol groups at the surface of an octanedithiol-SAM leads to selective nucleation. After an induction period during which the growth rate is rather slow, the deposition rate increases significantly, which has been attributed to the reaction of the precursor with previously deposited gold nuclei on top of the SAM.[13]

To investigate whether OMCVD presents a more universal method for the selective metallization of SAMs, we have started a systematic study using precursors for other metals. Our studies particularly focused on the deposition of palladium onto various functionalized SAMs using Cp(allyl)Pd as the precursor due to its high volatility (vapor pressure: 0.08 mbar at 30 °C[22]) and adequate stability toward air. In this paper, we report on the selective OMCVD of palladium onto thiol-, hydroxy-, and phenyl-terminated SAMs as well as on an hydroxy-terminated SAM modified by the reaction with TMAA prior to the deposition of palladium.

Experimental Details

Materials. 4-Biphenylthiol (BT) and 4,4′-biphenyldithiol (BDT) were synthesized from the corresponding sulfonyl chlorides by reduction with lithium aluminum hydride ($LiAlH_4$). The crude products were purified by sublimation.[23] Cyclopentadienyl-allyl-palladium (Cp(allyl)Pd) was synthesized from potassium tetrachloropalladate following standard procedures.[24,25] Trimethylamine alane (TMAA) was obtained from the reaction of $LiAlH_4$ with trimethylammonium chloride and purified by sublimation.[26] 1-Dodecanthiol (DT) and 11-mercaptoundecanol (MUD) were purchased from Aldrich and used without any further purification.

Sample Preparation. The Ag substrates for the XPS measurements were prepared by evaporation of 5 nm of titanium (99.8%, Chempur) followed by 100 nm of silver (99.99%, Aldrich) onto polished silicon wafers (Wacker silicone) using a commercial evaporator (Leybold Univex 300) at a base pressure of 10^{-6} mbar. The wafers were cut into 10 × 13 mm pieces for XPS measurements prior to the self-assembly process.

Self-assembled monolayers of BT and BDT were prepared by immersion of the silver substrates in a 1 mM solution of the aromatic thiols in dichloromethane for 20 h. In the case of BDT, an equimolar amount of *n*-tributylphosphine was added to prevent the formation of BDT multilayers on the surface.[27] For the preparation of DT and MUD monolayers, the silver substrates were immersed in a 1 mM solution of the corresponding thiol in ethanol for 20 h. After removal from the solution, the substrates were thoroughly rinsed with dichloromethane and dried in a stream of dry argon.

OMCVD Experiments. For the OMCVD of palladium, the SAMs and a small amount of Cp(allyl)Pd (∼15−20 mg) were placed in a glass tube, which was then evacuated using a rotary pump to a pressure of 10^{-2} mbar. The valve leading to the pump was closed and the glass tube was left at room temperature for 10 min to 8 h. After the tube was vented, the samples were thoroughly rinsed with dichloromethane and dried in a stream of dry argon.

For the deposition of TMAA, the SAMs were exposed to the vapor of TMAA for 20 s. Due to the high air and water sensivity of TMAA, all procedures involving TMAA were conducted under inert conditions either in a glovebox or with use of standard Schlenk techniques (H_2O and O_2 < 1 ppm). After the exposure to TMAA, the substrates were transferred to a glass tube, which was then evacuated for 20 min (10^{-2} mbar) to remove physisorbed material. It was carefully watched that the substrates did not come into contact with the ambient laboratory atmosphere to avoid extensive hydrolysis/oxidation of the Al−H bonds.

Analytical Methods. The XPS experiments were carried out using a modified Fisons X-ray photoelectron spectrometer equipped with a Al Kα X-ray source and a CLAM2 electron energy analyzer. The pass energy was set to 50 eV. The typical operating pressure was less than 10^{-8} mbar. All binding energies were referenced to the substrate signal, that is, the Ag $3d_{5/2}$ peak at 368.3 eV.

X-ray powder diffraction spectra were recorded on a Bruker-AXS D8 diffractometer. For the capillary measurements, a pinhole configuration was used with Cu Kα radiation, and a Goebel mirror with a parallel plate collimator combined with 0.1-mm divergence slits were placed in front of the detector.

(11) Käshammer, J.; Wohlfart, P.; Weiss, J.; Winter, C.; Fischer, R. A.; Mittler-Neher, S. *Opt. Mater.* **1998**, *9*, 406.
(12) Winter, C.; Weckenmann, U.; Fischer, R. A.; Käshammer, J.; Scheumann, V.; Mittler, S. *Chem. Vap. Deposition* **2000**, *6*, 199.
(13) Wohlfart, P.; Weiss, J.; Käshammer, J.; Winter, C.; Scheumann, V.; Fischer, R. A.; Mittler-Neher, S. *Thin Solid Films* **1999**, *340*, 274.
(14) Busse, S.; Käshammer, J.; Mittler-Neher, S. *Sensors Actuators B* **1999**, *20*, 148.
(15) Schreiber, F. *Prog. Surf. Sci.* **2000**, *65*, 151.
(16) Ulman, A. *Chem. Rev.* **1996**, *96*, 1533.
(17) Bain, C. D.; Whitesides, G. M. *Adv. Mater.* **1989**, *4*, 110.
(18) Reed, M. A.; Tour, J. M. *Sci. Am.* **2000**, *282*, 86.
(19) Bumm, L. A.; Arnold, J. J.; Cygan, M. T.; Dunbar, T. D.; Burgin, T. P.; Jones, L., II.; Allara, D. L.; Tour, J. M.; Weiss, P. S. *Science* **1996**, *271*, 1705.
(20) Reed, M. A.; Zhou, C.; Muller, C. J.; Burgin, T. P.; Tour, J. M. *Science* **1997**, *278*, 252.
(21) Zhou, C.; Deshpande, M. R.; Reed, M. A.; Jones, L., II.; Tour, J. M. *Appl. Phys. Lett.* **1997**, *71*, 611.
(22) Hierso, J.-C.; Serp, P.; Feurer, R.; Kalck, P. *Appl. Organomet. Chem.* **1998**, *12*, 161.
(23) Himmel, H. J.; Terfort, A.; Wöll, C. *J. Am. Chem. Soc.* **1998**, *120*, 12069.
(24) Zhang, Y.; Yuan, Z.; Puddephatt, R. J. *Chem. Mater.* **1998**, *10*, 2293.
(25) Tatsuno, Y.; Yoshida, T.; Otsuka, S. *Inorg. Synth.* **1979**, *19*, 220.
(26) Ruff, J. K.; Hawthorne, M. F. *J. Am. Chem. Soc.* **1960**, *82*, 2141.
(27) Weckenmann, U.; Mittler, S.; Naumann, K.; Fischer, R. A. *Langmuir* **2002**, *18*, 5479.

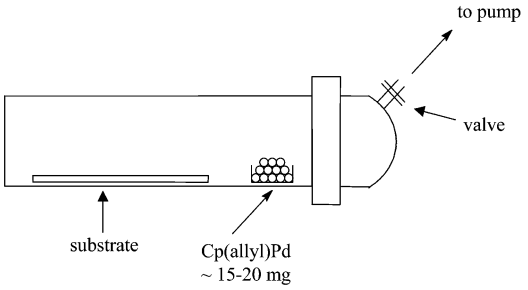

Figure 1. Sketch of the glass vessel used for the OMCVD of palladium. After the substrates and the precursor were placed in the glass vessel, it was evacuated using a rotary pump. The valve to the pump was closed after 30 s and the OMCVD was carried out under static vacuum conditions.

Table 1. Selected Bond Lengths [Å] and Angles [deg] for the Dimeric (Allyl)(*p*-cresolthiolato)palladium

Bond Lengths					
Pd(1)−S(1)	2.361(3)	Pd(2)−S(1)	2.363(3)	Pd(1)−S(2)	2.378(3)
Pd(2)−S(2)	2.364(3)	Pd(1)−C(2)	2.071(12)	Pd(2)−C(5)	2.13(2)
Pd(1)−C(1)	2.170(12)	Pd(2)−C(4)	2.224(13)	S(1)−C(7)	1.773(12)
S(2)−C(14)	1.771(11)	C(7)−C(8)	1.418(16)	C(7)−C(12)	1.359(15)

Bond Angles			
S(1)−Pd(1)−S(2)	83.38(10)	S(1)−Pd(2)−S(2)	83.61(11)
S(2)−Pd(1)−C(1)	173.3(4)	S(2)−Pd(2)−C(4)	172.0(5)
C(7)−S(1)−Pd(1)	111.6(3)	C(7)−S(1)−Pd(2)	110.8(4)
C(14)−S(2)−Pd(1)	111.1(4)	C(14)−S(2)−Pd(2)	112.2(4)
Pd(1)−S(1)−Pd(2)	85.44(11)	Pd(1)−S(2)−Pd(2)	85.04(10)
C(1)−C(2)−C(3)	132.9(18)	C(4)−C(5)−C(6)	140(3)

X-ray Single-Crystal Structure Analysis. Measurements were performed on a Bruker AXS SMART 100 diffractometer. Graphite-monochromated Mo Kα radiation (0.71073 Å) was used. The structures were solved with direct methods and refined anisotropically with the program SHELX-97. Parameters were refined against F^2. The R values are defined as R1 $= (\sum(|F_o| - |F_c|)/\sum(|F_c|)$ and R2 $= \{\sum[w(F_o^2 - F_c^2)^2]/[w(|F_c|^2)^2]\}^{1/2}$. Solid-state structure of (a) (allyl)(*tert*-butylthiolato)palladium (see supplementary figure) and (b) (allyl)(*p*-cresolthiolato)-palladium complexes is shown in Figure 11. Selected bond lengths/bond angles of complex (b) are summarized in Table 1.

Results

Organometallic Vapor Deposition of Palladium onto a BDT-SAM. The OMCVD of palladium onto BDT-SAMs was conducted at room temperature in an evacuated glass vessel under static vacuum conditions (Figure 1) at $\sim 10^{-2}$ mbar (the reported vapor pressure of Cp(allyl)Pd is 4×10^{-2} mbar at room temperature).[22] Figure 2 shows the XP spectra of the Pd 3d region taken of the samples after deposition times varying from 10 min to 8 h. The appearance of a Pd 3d signal indicates that deposition of palladium occurred. The peak intensity which correlates with the amount of palladium present on the surface was plotted against the deposition time (Figure 3), revealing the presence of two distinct growth regimes: For deposition times from 10 min to 2 h, the peak intensity does not increase and the amount of palladium on the surface remains constant within the measuring error. However, if the deposition time exceeds 2 h, a steady increase in the Pd 3d peak intensity was observed. A closer inspection of the XP spectra of the Pd 3d region reveals that, during the initiation period of the growth, only one palladium species is present on the surface, giving rise to a signal located at 337.3 eV with respect to its Pd

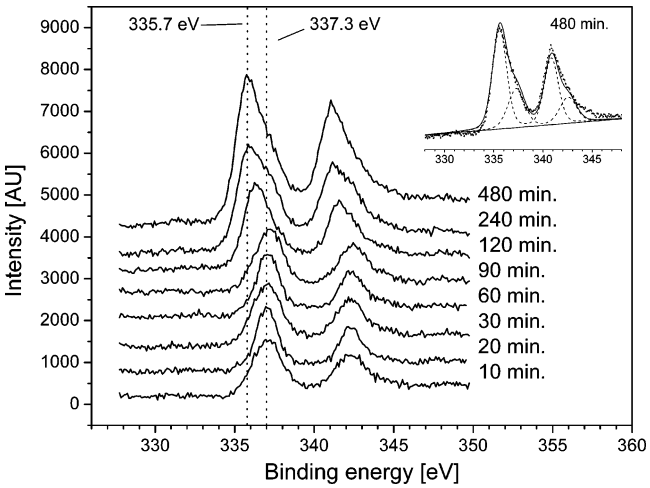

Figure 2. Pd 3d doublet of a BDT-SAM after the OMCVD of palladium at room temperature and 10−2 mbar for deposition times from 10 to 480 min. The inset shows the fitted spectrum after a deposition time of 480 min, which exhibits two distinct signals at 337.3 and 335.7 eV with respect to the Pd $3d_{5/2}$ component.

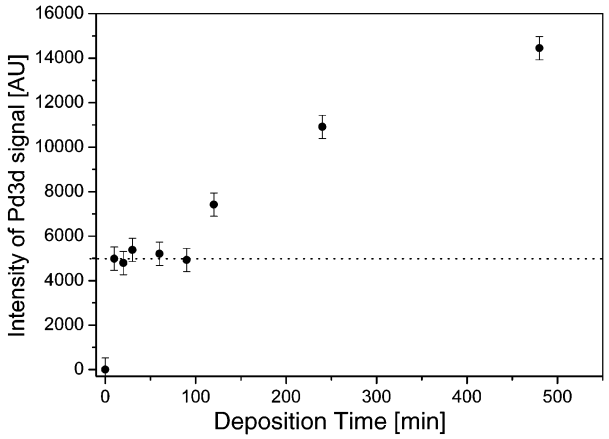

Figure 3. Plot of the peak intensity of the Pd 3d signal detected on a BDT-SAM after the OMCVD of palladium against the deposition time.

$3d_{5/2}$ component. The increase of the peak intensity after a deposition time of 2 h is accompanied by the appearance of a second Pd 3d signal with its Pd $3d_{5/2}$ component located at 335.5 eV. The intensity of the second signal increases with deposition time while the intensity of the first Pd 3d signal remains constant (Figure 2).

Since Cp(allyl)Pd is easily reduced by hydrogen, a BDT-SAM which had been exposed to the vapor of Cp-(allyl)Pd for 20 min and the XP spectrum of which exhibited a single Pd 3d signal at 337.3 eV was treated with hydrogen for 60 min at room temperature. It was observed that this treatment had no effect on the position of the Pd 3d signal observed on the BDT-SAM prior to the exposure to hydrogen.

Figure 4 shows the S 2p region of the XP spectrum obtained from a BDT-SAM before and after the deposition of palladium. The shape of the signal and the peak position are independent of the deposition time. As an example, the spectrum obtained from a BDT substrate after a deposition time of 60 min is shown. For the peak fit, the energy difference between the S $2p_{1/2}$ and S $2p_{3/2}$ components was set to 1.2 eV and their intensity ratio was set to 1:2.[28] In the spectrum of a BDT-SAM prior

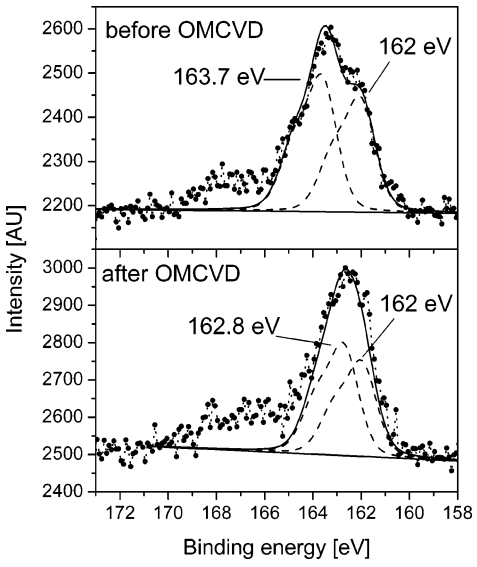

Figure 4. S 2p doublet of a BDT-SAM before and after the OMCVD of palladium for 60 min. The S 2p signal at 163.7/164.9 eV assigned to the free thiol groups at the surface of the BDT-SAM is shifted to 162.8/164.0 eV upon the deposition of palladium.

to the deposition of palladium, two S 2p doublets with their S $2p_{3/2}$ component located at 162.0 and 163.6 eV were observed, which agrees well with the reported shifts of the S $2p_{3/2}$ signal for sulfur atoms in thiolate−silver (S−Ag) bonds and free thiol groups (S−H), respectively.[29] The intensity ratio of the two signals is in agreement with the expected ratio for an ordered BDT-SAM in which the 4,4′-axis of the molecules is oriented perpendicular to the silver surface.[27] After the deposition of palladium, the signal of the thiol groups exposed at the surface of the SAM has shifted from 163.6 to 162.7 eV, indicating a change in the chemical environment whereas the peak position of the signal at 162.0 eV assigned to sulfur in S−Ag bonds at the surface of the silver substrate remained unchanged. The quantitative analysis of the S 2p and Pd 3d peak intensities after deposition times below 2 h provides a value of 1:1.5 ± 0.2 for the Pd/S ratio (from the S 2p peak intensity only the component originating from sulfur in S−Pd bonds was considered).

Selectivity of the Palladium Deposition. To investigate the selectivity of the OMCVD process, a BT-SAM which exhibits a less reactive, most likely passive, phenyl-terminated surface was placed together with a BDT-SAM in the deposition vessel and subjected to the OMCVD of palladium at room temperature under static vacuum conditions for (a) 30 min and (b) 3 h. The XP spectra of the Pd 3d region are presented in Figure 5. After a deposition time of 30 min, a Pd $3d_{5/2}$ signal at 337.3 eV was observed on the BDT-SAM only whereas no deposition occurred on the BT-SAM. However, when the exposition time was extended to 3 h, a Pd 3d signal appeared in the spectra of both the BT- and the BDT-SAM, indicating the unselectivity of the deposition at this stage. A closer inspection of the Pd 3d signals reveals that in the case of the BT-SAM only one Pd 3d species is present on the surface, giving rise to a Pd 3d signal with its Pd $3d_{5/2}$ component located at 335.5 eV. In contrast, a superposition of two signals can be observed in the spectrum of the BDT-SAM, which is in agreement with the results presented in the previous section.

Furthermore, we observed that, as was the case with a BT-SAM, for reasonably short deposition times (<3 h) no deposition occurred on an OH-terminated SAM formed from 11-mercaptoundecanol (MUD) either.

Activation of Inert OH-Terminated SAMs for the Deposition of Palladium. *Reduction of Cp(allyl)Pd Using TMAA.* Prior to the OMCVD experiments, the reactivity of TMAA toward Cp(allyl)Pd was tested by adding a solution of the precursor in *n*-pentane to a solution (*n*-pentane) containing an equimolar amount of TMAA. Immediately upon mixing the components, a black precipitate formed. After filtration, the residual black powder was washed with diethyl ether, dried, and analyzed by XRD (Figure 6). Three broad reflections with values for 2θ of 40.3°, 46.1°, and 68° can be observed in the resulting spectrum, which are in agreement with the reported values for cubic palladium at

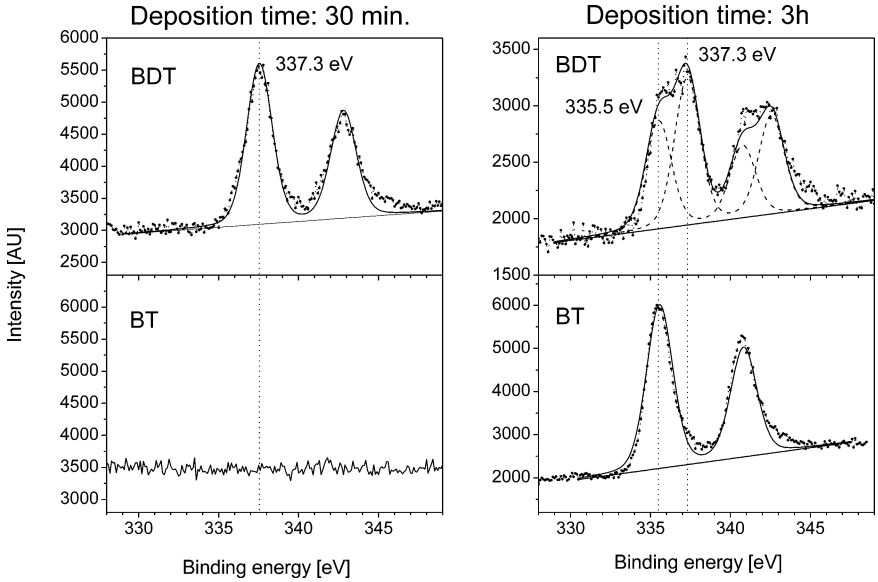

Figure 5. XP spectra of the Pd 3d region of a BT and a BDT-SAM after the OMCVD of palladium for 30 min (left side) and 3 h (right side). The signal at 337.3 eV is assigned to Pd(II) whereas the signal at 335.5 eV can be ascribed to Pd(0).

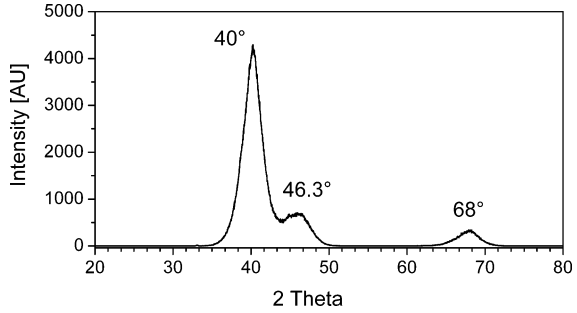

Figure 6. XRD spectrum of polycrystalline palladium obtained from the reaction of Cp(allyl)Pd with TMAA in *n*-pentane.

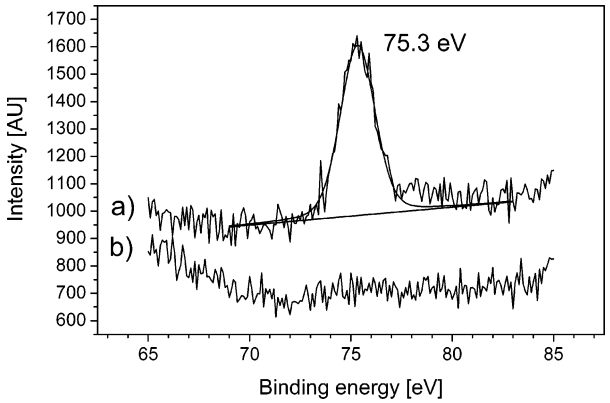

Figure 7. XP spectra of the Al 2p region of a MUD-SAM (a) and a DT-SAM (b) after the exposure of the SAMs to the vapor of TMAA for 20 s under inert conditions and the subsequent exposure to the vapor of Cp(allyl)Pd for 90 min.

40.1°, 46.7°, and 68.1°.[30] Reflections of aluminum and palladium/aluminum alloys as likely side products were not observed. It is well-known that organometallic compounds can be reduced by metal hydrides, yielding the pure transition metals or in some cases even the intermetallic alloys. It is therefore not surprising that TMAA is a suitable reagent for the reduction of Cp(allyl)Pd to Pd(0).

Selective OMCVD of Palladium onto an Alane-Activated Hydroxy-Terminated SAM. A DT- and a MUD-SAM were exposed to the vapor of TMAA for 20 s in the same reaction vessel. Previous studies have shown that this procedure results in the selective deposition of TMAA on an hydroxy-functionalized SAM.[31] The modified MUD- and the DT-SAM as well as a pure MUD-SAM were then subjected to the OMCVD of palladium at room temperature for 90 min following the procedure described for the deposition onto BT- and BDT-SAMs. Afterward, the samples were rinsed with dichloromethane and analyzed by XPS. The XP spectra of the Al 2p and Pd 3d region (Figures 7 and 8) reveal the presence of aluminum as well as palladium on the alane-modified MUD-SAM indicated by the appearance of the Al 2p signal at 75.2 eV and the Pd 3d signal at 336.1 eV. In contrast, neither of these peaks can be observed on the unmodified MUD- and the DT-SAM,

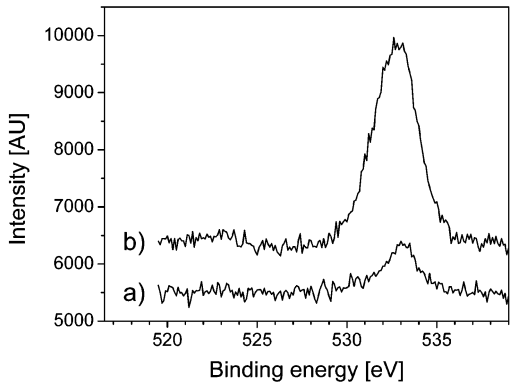

Figure 8. XP spectra of the Pd 3d region of a MUD-SAM modified with TMAA (a), a DT-SAM (b), and an unmodified MUD-SAM (c) after exposure to the vapor of Cp(allyl)Pd for 90 min.

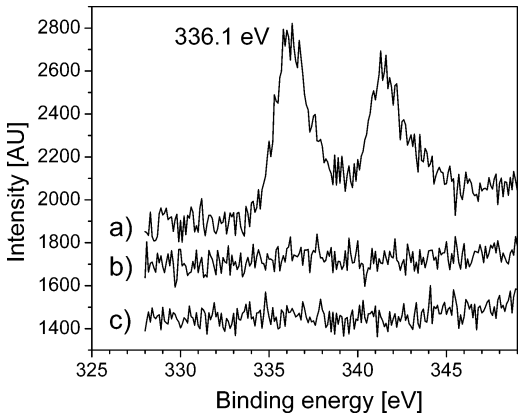

Figure 9. O 1s singlet of a MUD-SAM before (a) and after (b) the adsorption of TMAA and the OMCVD of palladium.

verifying the selectivity of the adsorption of TMAA and the subsequent deposition of palladium. It should be noted that a comparison of the O 1s signal of a pure MUD-SAM and a MUD-SAM after the deposition of TMAA and palladium shows that the peak intensity after the deposition process is 5 times larger than before (Figure 9), indicating that a considerable amount of oxygen other than the oxygen in the hydroxy groups of the MUD-SAM is present on the surface.

Discussion

OMCVD of Palladium onto SAMs Formed of BDT and BT. The investigation of the palladium OMCVD on SAMs formed of BDT and BT reveals that the deposition proceeds via two different growth mechanisms: Initially, a very rapid reaction of the gaseous precursor Cp(allyl)Pd with the free thiol groups exposed at the surface of the BDT-SAM takes place, leading to the appearance of a Pd 3d signal at 337.3 eV, whereas no deposition occurs on a BT-SAM. The Pd 3d signal at 337.3 eV, which can be observed in the XP spectrum of the BDT-SAM after short deposition times (<2 h), is within the range of the reported value of 337.7 ± 0.3 eV for the Pd 3d signal in Pd(II)−dithiolates,[32] indicating the deposition of a Pd(II) species rather than Pd(0) on the SAM.

(28) Scofield, J. H. *J. Electron Spectrosc.* **1976**, *8*, 129.
(29) Bensebaa, F.; Zhou, Y.; Deslandes, Y.; Kruus, E.; Ellis, T. H. *Surf. Sci.* **1998**, *405*, L472.
(30) Kern, A.; Eysel, W. JCPDS, Powder Diffraction File, ICDD, 1993.
(31) Weiss, J.; Himmel, H.-J.; Fischer, R. A.; Wöll, C. *Chem. Vap. Deposition* **1998**, *4*, 17.
(32) Moulder, J. F.; Stickle, W. E.; Sobol, P. E.; Bomben, K. D. *Handbook of X-ray Photoelectron Spectroscopy*; Perkin-Elmer Corporation: Eden Prairie, MN, 1992.

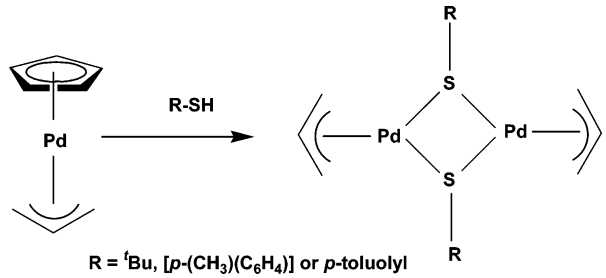

Figure 10. Schematic reaction of Cp(allyl)Pd with *p*-thiocresol and *tert*-butylthiol, leading to the formation of dimeric palladiumthiolato complexes.

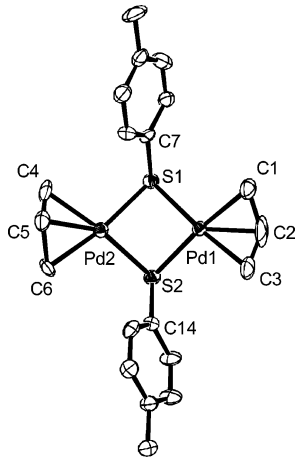

Figure 11. X-ray structure of the dimeric (allyl)(*p*-cresolthiolato)palladium complex obtained by the reaction of Cp(allyl)Pd with *p*-thiocresol.

Additionally, the reaction of the precursor with the thiol groups of the SAM surface results in a shift of the S $2p_{3/2}$ signal at 163.7 eV ascribed to the sulfur atoms in surface thiol groups to a S $2p_{3/2}$ signal at 162.8 eV. The exact value of the S 2p signal of sulfur atoms in a Pd−S bond has not been reported in the literature yet, but it is well-known that sulfur atoms in metal thiolate bonds give rise to a S 2p signal located at lower binding energies compared to sulfur atoms in free thiol groups. Therefore, it is reasonable to assign the observed S 2p signal at 162.8 eV to sulfur atoms in Pd−thiolate bonds. The early stages of the OMCVD of palladium onto a BDT-SAM can be described as a self-limiting process since neither the position nor the intensity of the Pd 3d signal exhibit any changes with deposition time ($t < 2$ h). From the value of 1:1.5 ± 0.3 for the ratio Pd/S obtained from the quantitative analysis of the XP spectra during this period it can be concluded that most likely a Pd(II) monolayer forms on the surface of the BDT-SAM within 10 min, in which the Pd(II) species are bound to the SAM surface via either one or two Pd−S bonds. The Pd(II)-covered SAM surface is then stable against any further deposition of palladium for 2 h, even if the surface is treated with hydrogen.

To explain this observation, we tested the reactivity of Cp(allyl)Pd toward various thiols in solution and found that dimeric (allyl)(*μ*-thiolato)palladium species were quantitatively formed according to Figure 10. Figure 11 depicts the structure of dimeric (allyl)(*p*-cresolthiolato)palladium complex obtained by single-crystal X-ray diffraction studies. Similar species have been reported to form upon the addition of a thiol to a solution of dimeric (allyl)palladium-chloride and the structures have been discussed elsewhere.[33,34] The reactivity of these compounds toward hydrogen was tested by bubbling hydrogen through a solution of the complexes in dichloromethane for 60 min at room temperature. In contrast to Cp(allyl)Pd, which is readily reduced under these conditions and forms Pd(0), no change was observed for the (allyl)(*μ*-thiolato)palladium complexes; that is, they are stable against hydrogen. It is assumed that a similar reaction takes place between Cp(allyl)Pd and the free thiol groups at the SAM−gas interface, which would yield a allyl-terminated surface (Figure 12). This model would explain the passivation of the BDT-SAM after the initial formation of a Pd(II) layer and its unreactivity toward hydrogen. However, we do not have any direct proof for the presence of allyl groups on the SAM surface so far.

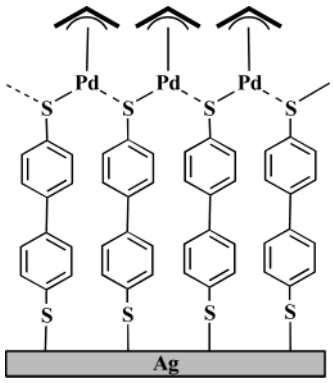

Figure 12. Proposed structure of the Pd(II) covered surface of a BDT-SAM after the exposure of a BDT-SAM to the vapor of Cp(allyl)Pd for $t < 2$ h at room temperature. Dashed lines indicate coordinative bonds, just for electron-counting roles in coordination chemistry. The formed oxidation state of Pd is +1.

Extending the deposition time to more than 2 h (at room temperature) or increasing the deposition temperature (while keeping the deposition time below 2 h) leads to the nonselective deposition of palladium as indicated by the appearance of a Pd 3d signal at 335.5 eV in the XP spectra of both the BDT- and the BT-SAM. According to the literature, Pd(0) gives rise to a Pd 3d signal with its Pd $3d_{5/2}$ component located at 335.0 eV; that is, the observed value for Pd(0) is shifted to a higher binding energy by 0.5 eV, which is above the experimental error of 0.2 eV. Most likely, the origin of this shift is associated with the Coulomb interaction between an emitted photoelectron and a hole remaining behind in the palladium particles.[35] The hole will be annihilated by the substrate, but the rate of this process depends on the resistance between the substrate and the particle. Since the BT and BDT molecules increase the resistance between substrate and particle, the hole in the palladium particle will exist long enough to influence the energy of the emitted electron, leading to a shift of the binding energy to a higher value.

The nonselective deposition of Pd(0) upon extending the deposition time or increasing the deposition tem-

(33) Singhal, A.; Jain, V. K.; Mishra, R.; Varghese, B. *J. Mater. Chem.* **2000**, *10*, 1121.
(34) Redon, R.; Cramer, R.; Bernes, S.; Morales, D.; Torrens, H. *Polyhedron* **2001**, *20*, 3119.
(35) Ohgi, T.; Sheng, H.-Y.; Dong, Z.-C.; Nejoh, H.; Fujita, D. *Appl. Phys. Lett.* **2001**, *79*, 2453.

perature can be explained by the thermal instability of Cp(allyl)Pd. The precursor decomposes slowly upon exposure to room temperature and the decomposition rate increases with rising temperature. Therefore, it is not surprising that nonselective deposition on both the BT-SAM and Pd(II)-covered BDT-SAM takes place at extended deposition times and higher deposition temperatures since both are a result of the parasitic decomposition of the thermally labile precursor on any surface and in the gas phase.

Selective OMCVD of Pd(0) onto an Alane-Activated MUD-SAM. To selectively deposit Pd(0) on SAMs, a suitably functionalized SAM had to be found which does not react with Cp(allyl)Pd to form Pd(II) since this obviously leads to a self-terminating growth mechanism. Since the decomposition of Cp(allyl)Pd follows an autocatalytic pathway, the presence of Pd(0) on the surface will catalyze further deposition of palladium, thereby leading to the selective deposition of Pd(0). The idea was to first activate a passive SAM by the pre-deposition of a reducing agent which then allows the conversion of Pd(II) into Pd(0). Hydroxy-terminated SAMs are passive against the deposition of Cp(allyl)Pd at room temperature. However, TMAA, a well-established precursor for the CVD of aluminum,[36] is known to selectively bind to OH-terminated SAMs, forming a triple layer of AlH_3 units as we have shown previously.[31] Thus, the modification of an hydroxy-terminated SAM with TMAA presents a promising approach since TMAA is a suitable reagent for the reduction of Cp(allyl)Pd, which is demonstrated by the rapid reaction of TMAA with the precursor to form Pd(0).

The results presented in this paper confirm that the results of this study can be transferred to the adsorption of TMAA on SAMs formed on silver. TMAA was selectively attached to an hydroxy-functionalized MUD-SAM on silver by exposure to the vapor of TMAA whereas deposition is inhibited on a methyl-terminated DT-SAM. The attachment of TMAA presumably proceeds via protolysis of one or two Al−H bonds by hydroxy groups exposed at the surface of the MUD-SAM, resulting in an Al−O linkage between the surface and TMAA. Previous studies have revealed that initially a multilayer of Al−H-linked AlH_3 units forms on the top of the first layer, which can be removed except for one bilayer by exposure to UHV for 12 h at room temperature. In the present case, the alane-activated MUD-SAMs were not treated under UHV conditions and most likely an ill-defined multilayer of Al−H/Al−OH units has formed on the surface of the SAM due to partial hydrolysis. However, it is reasonable to assume that a sufficient number of Al−H bonds for the effective reduction of Cp(allyl)Pd is present on the surface.

The exposure of the TMAA-modified MUD-SAM to the vapor of Cp(allyl)Pd at room temperature leads to the deposition of palladium as revealed by the appearance of a Pd 3d signal in the XP spectrum. No deposition of palladium occurs on a DT-SAM and an unmodified MUD-SAM, reflecting the low reactivity of Cp(allyl)Pd toward hydroxy groups. A single Pd 3d signal was observed in the XP spectrum of the alane-modified MUD-SAM located at 336.1 eV, exceeding the reported value for Pd(0) by 1.1 eV. However, this value is still considerably lower than the value of 337.3 eV, which was observed after the deposition of a Pd(II) monolayer on a BDT-SAM. As in the case of the deposition of Pd(0) onto a BT- and a BDT-SAM, most likely Coulomb interactions between the deposited palladium and the emitted electron are responsible for the shift of the Pd(0) signal toward a higher binding energy. Compared to the deposition of palladium on the BT- and BDT-SAMs, the resistance between the substrate and the palladium particles is increased by an inorganic layer containing aluminum oxide and hydroxide (indicated by the large amount of oxygen present on the surface) in addition to the underlying SAM. Since both layers show poor conductive properties and contribute to the total resistance between particles and substrate, it is not surprising that the resulting Pd 3d signal is shifted to a higher binding energy than in the case of the palladium deposition on nonmodified BT- and BDT-SAMs. The large amount of oxygen present on the surface after the deposition of TMAA and Pd(0) indicates that hydrolysis of Al−H bonds on the surface has taken place during the experiment. For a detailed study of the mechanism of the deposition and the resulting structure, it will therefore be necessary to carry out the activation of the SAM surface with TMAA as well as the deposition of palladium under UHV conditions and to analyze the substrates without exposing them to the ambient atmosphere.

Nevertheless, we have shown that it is possible to turn the passive surface of the MUD-SAM into a highly reactive surface by the adsorption of TMAA, which then allows the selective deposition of Pd(0).

Conclusions

It has been shown that the room temperature OMCVD of palladium using Cp(allyl)Pd as a precursor onto SAMs formed of BDT and BT on silver initially results in the self-limiting selective deposition of a Pd(II) monolayer on a BDT SAM in which the Pd(II) species are bound to the SAM surface via Pd−S bonds. The structure of the resulting surface is thought to closely resemble the molecular structure of dimeric palladiumthiolato complexes formed by the reaction of Cp(allyl)Pd with thiols in solution. Upon extension of the deposition time or by increasing the deposition temperature, Cp(allyl)Pd shows parasitic, nonselective decomposition due to its low thermal stability and leads to the nonselective deposition of elemental palladium on both the BT-SAM and the Pd(II) covered surface of the BDT SAM. The selective deposition of Pd(0) was achieved by TMAA activation of a MUD-SAM on silver. By this procedure, the surface of the MUD-SAM, which does not promote the deposition of palladium, was turned into a reactive surface due to the presence of highly reactive Al−H bonds on the SAM surface, which are capable of reducing Cp(allyl)Pd to Pd(0). In summary, our results show that there are many interesting possibilities to play around with the surface reactivity of SAMs toward well-established CVD and OMCVD precursors, realizing the selective deposition of metallic structures or even more complex architectures at very mild conditions on organic surfaces. It is quite likely that the composition and the structural quality of the metallized SAMs we

(36) Gladfelter, W. L.; Boyd, D. C.; Jensen, K. F. *Chem. Mater.* **1989**, *1*, 339.

have described here can be much improved if UHV techniques are employed.

Acknowledgment. We thank the Degussa AG for a donation of potassium tetrachloropalladate. U. Weckenmann thanks the Graduierten Kolleg "Dynamische Prozesse an Festkörperoberflächen" for a fellowship.

Supporting Information Available: X-ray structure of the dimeric (allyl)(*tert*-butylthiolato)palladium complex and tables of crystallographic data (PDF). This material is available free of charge via the Internet at http://pubs.acs.org.

CM031094P